WHOLESALE BANKING

Calibration of Stochastic Convenience Yield Models for Crude Oil Using the Kalman Filter

WHOLESALE BANKING

Calibration of Stochastic Convenience Yield Models for Crude Oil Using the Kalman Filter

Adriaan Krul 3 July 2008 adriaan.krul@ingbank.com

Agenda

1. Introduction

Every year over 600 million contracts are traded on different boards.

- Chicago Board Of Trade,
- New York Cotton Exchange,
- New York Merchantile Exchange.

A futures contract is a contract, traded on a futures exchange, to buy or sell a certain underlying instrument at a certain date in the future, at a specified price. This price is called the future price and is denoted by

$$F(t,T), \tag{1}$$

with t the current time and T the maturity time.

Futures prices are simply given by

$$F(t,T) = S_t e^{\int_t^T (r-\delta_s)ds}, \tag{2}$$

with S_t the spot price, r the risk-free interest rate and δ_t the convenience yield.

Convenience yield is the premium associated with holding an underlying product or physical good, rather than the contract or derivative product.

Both spot price and convenience yield are believed to have stochastic processes.

Problem:

These processes are not observable in the market.

Solution:

Use of the Kalman filter.

2. Initial stochastic processes

2.1. Convenience yield follows an Ornstein-Uhlenbeck process (OU)

Empirical evidence shows that the convenience yield follows a mean-reverting pattern, i.e.

$$d\delta_t = k(\alpha - \delta_t)dt + \sigma_\delta dW_t^\delta,$$

and for the spot price we have a geometrical Brownian motion,

$$dS_t = (\mu - \delta_t)S_t dt + \sigma_S S_t dW_t^S,$$

- α is the long rate mean to which δ_t tends to revert
- k is the speed of adjustment
- μ is the drift term
- σ_S and σ_δ are the volatilities of dS_t and $d\delta_t$ respectively
- $dW_t^\delta dW_t^S = \rho dt$, ρ is the correlation term.

2.2. Convenience yield follows a Cox-Ingersoll-Ross process (CIR)

$$\begin{cases} \dfrac{dS_t}{S_t} = (\mu - \delta_t)dt + \sigma_S \sqrt{\delta_t} dW_t, \\ d\delta_t = k(\alpha - \delta_t)dt + \sigma_\delta \sqrt{\delta_t} dZ_t. \end{cases} \tag{3}$$

In this way, the convenience yield can not be negative. However, as we shall see later, the CIR process gives very unaccurate results. For both the OU and the CIR process for the convenience yield and the GBM for the spot price we can get a closed form solution for the future prices.

3. Closed form solution of the futures prices

Considering the OU process as the intial stochastic process for the convenience yield and a GMB for the spot price we can derive the closed form solution of the future prices explicitly by assuming an affine form, i.e.

$$F_t(S, \delta, \tau) = S_t e^{A(\tau) - B(\tau)\delta_t}, \tag{4}$$

where

$$A(\tau) = \left[\left(r - \tilde{\alpha} + \frac{\sigma_\delta^2}{2k^2} - \frac{\sigma_S \sigma_\delta \rho}{k}\right)\tau\right] + \left[\frac{\sigma_\delta^2}{4}\frac{1 - e^{-2k\tau}}{k^3}\right] + \left[\left(\tilde{\alpha}k + \sigma_\delta \sigma_S \rho - \frac{\sigma_\delta^2}{k}\right)\left(\frac{1 - e^{-k\tau}}{k^2}\right)\right]$$

and

$$B(\tau) = \frac{1 - e^{-k\tau}}{k}, \quad \tilde{\alpha} = \alpha - \frac{\lambda}{k},$$

By looking at equation (4) we see that the futures prices are linear in the log of the state variable S_t. As we shall see, this comes in handy when applying the Kalman filter. A similar form exists for the furture prices if the convenience yield follows a CIR process.

4. The Kalman filter

The main idea of the Kalman filter is to use observable variables to reconstitute the value of the non-observable variables (the spot price and convenience yield). Since the futures prices are widely observed and traded in the market, we consider these our observable variables.

In state variable terms, we have in combination with $x_t = \ln S_t$,

$$\ln F_t(\tau) = x_t + A(\tau) - B(\tau)\delta_t + \epsilon_t. \tag{5}$$

The error term ϵ_t has a diagonal variance matrix $\mathbf{H}$.

In combination with the relationship $x_t = \ln S_t$ we have

$$\begin{cases} dx_t = (\mu - \delta_t - \dfrac{1}{2}\sigma_S^2)dt + \sigma_S dW_t^S, \\ d\delta_t = k(\alpha - \delta_t)dt + \sigma_\delta dW_t^\delta. \end{cases} \tag{6}$$

From (6) the transition equation follows immediately,

$$\begin{bmatrix} x_{t_i} \\ \delta_{t_i} \end{bmatrix} = \begin{bmatrix} (\mu - \frac{1}{2}\sigma_S^2)\Delta t \\ k\alpha\Delta t \end{bmatrix} + \begin{bmatrix} 1 & -\Delta t \\ 0 & 1 - k\Delta t \end{bmatrix} \begin{bmatrix} x_{t_{i-1}} \\ \delta_{t_{i-1}} \end{bmatrix} + \begin{bmatrix} 1 & 0 \\ 0 & 1 \end{bmatrix} \begin{bmatrix} \xi_{t_i}^1 \\ \xi_{t_i}^2 \end{bmatrix}, \tag{7}$$

where $\boldsymbol{\xi}_{t_i}$ takes into account the Brownian motions dW_t^S and dW_t^δ. $\boldsymbol{\xi}_{t_i}$ is assumed normal with mean zero and has a covariance-variance matrix given by

$$\mathbf{V}_{t_i} = \begin{bmatrix} \sigma_S^2\Delta t & \rho\sigma_\delta\sigma_S\Delta t \\ \rho\sigma_\delta\sigma_S\Delta t & \sigma_\delta^2\Delta t \end{bmatrix} \tag{8}$$

Note that the covariance-variance matrix does not depend on the state variables.

A similar procedure can be done in the case of the CIR process. However, the covariance-variance matrix does now depend on the state variable δ_t which will cause problems as we will see later.

$$\mathbf{V}_{t_i} = \begin{bmatrix} \sigma_S^2 \Delta t \delta_{t_{i-1}} & \rho\sigma_S\sqrt{\Delta t}\sqrt{\delta_{t_{i-1}}}\sqrt{\mathbb{V}\mathrm{ar}[\delta_{t_i}|\delta_{t_{i-1}}]} \\ \rho\sigma_S\sqrt{\Delta t}\sqrt{\delta_{t_{i-1}}}\sqrt{\mathbb{V}\mathrm{ar}[\delta_{t_i}|\delta_{t_{i-1}}]} & \mathbb{V}\mathrm{ar}[\delta_{t_i}|\delta_{t_{i-1}}] \end{bmatrix},$$

where

$$\mathbb{V}\mathrm{ar}[\delta_{t_i}|\delta_{t_{i-1}}] = \alpha(\frac{\sigma_\delta^2}{2k})(1-e^{-k\Delta t})^2 + \delta_{t_{i-1}}(\frac{\sigma_\delta^2}{k})(e^{-k\Delta t} - e^{-2k\Delta t}). \quad (9)$$

5. Iterative procedure

We now have a measurement equation and a transition equation that depend on the latent state variables S_t and δ_t and on the observed variables, the futures prices F_t.

$$\varphi = \left\{ k, \mu, \alpha, \lambda, \sigma_S, \sigma_\delta, \rho, \{h_j\}_{j=1}^{n} \right\}.$$

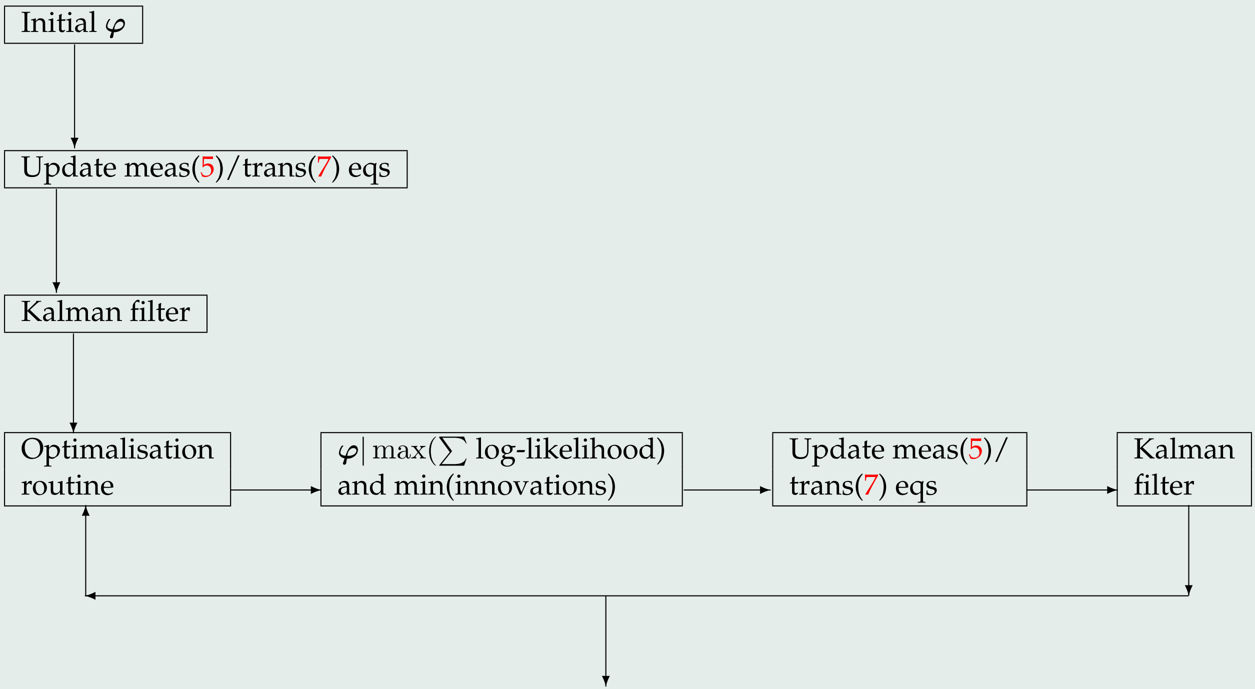

$$\text{Optimized parameter set} = \varphi$$

This optimized parameter set is used for the last time to update the matrices in both the measurement and transition equation to generate the paths of the futures prices and the convenience yield.

6. Numerical results for the Ornstein-Uhlenbeck process for the commodity light crude oil

We use weekly observations of the light crude oil market from 01-02-2002 until 25-01-2008 (313 observations). At each observation we consider 7 monthly contracts.

6.1. Details for starting the iterative procedure

- The nearest future price is retained as the spot price S_0.

- The δ_0 is subtracted out of two futures contracts at $t = 0$.

$$[\quad \mu \quad \sigma_S \quad \alpha \quad k \quad \sigma_\delta \quad \rho \quad \lambda \quad h1 \quad h2 \quad h3 \quad h4 \quad h5 \quad h6 \; h7];$$

```
lowerbound=[ -10  0.001   -10   0.001  0.001  -1    -10   -1 -1 -1 -1 -1 -1 -1];
upperbound=[  10     10    10      10     10   1     10    1  1  1  1  1  1  1];
```

Numerical results for the Ornstein-Uhlenbeck process for the commodity light crude oil

Prs	Ini parset	Opti parset	Ini parset	Opti parset	Ini parset	Opti parset
k	0.3	1.4221 (0.0372)	0.3	1.4221 (0.0380)	2	1.4221 (0.0382)
μ	0.2	0.3733 (0.1471)	0.2	0.3733 (0.1376)	0.2	0.3733 (0.1382)
α	0.06	0.0699 (0.1128)	0.2	0.0699 (0.1025)	0.06	0.0699 (0.1082)
λ	0.01	-0.0183(0.1602)	0.1	-0.0183(0.1459)	0.01	-0.0183(0.1543)
σ_S	0.4	0.3630 (0.0137)	0.4	0.3630 (0.0139)	0.5	0.3630 (0.0153)
σ_δ	0.4	0.4028 (0.0165)	0.4	0.4028 (0.0172)	0.4	0.4028 (0.0181)
ρ	0.8	0.8378 (0.0162)	0.5	0.8378 (0.0164)	0.5	0.8378 (0.0177)
$\|h_1\|$	0.0246	0.0188 (0.0008)	0.0246	0.0188 (0.0007)	0.01	0.0188 (0.0007)
$\|h_2\|$	0.0268	0.0072 (0.0003)	0.0268	0.0072 (0.0003)	0.01	0.0072 (0.0003)
$\|h_3\|$	0.0291	0.0022 (0.0001)	0.0291	0.0022 (0.0001)	0.01	0.0022 (0.0001)
$\|h_4\|$	0.0313	0.0000 (0.0001)	0.0313	0.0000 (0.0001)	0.01	0.0000 (0.0001)
$\|h_5\|$	0.0336	0.0006 (0.0000)	0.0336	0.0006 (0.0000)	0.01	0.0006 (0.0000)
$\|h_6\|$	0.0357	0.0000 (0.0001)	0.0357	0.0000 (0.0001)	0.01	0.0000 (0.0001)
$\|h_7\|$	0.0377	0.0014 (0.0001)	0.0377	0.0014 (0.0001)	0.01	0.0014 (0.0001)
Log-Likelihood		8744.6479		8744.6479		8744.6479

Table 1: Optimized parameter set (Opti parset) for different initial parameter sets (Ini parset). Standard errors in parentheses.

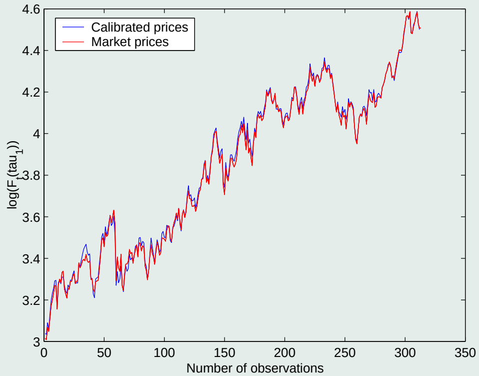

Figure 1: Comparison between the calibrated future prices and market future prices for contract τ_1.

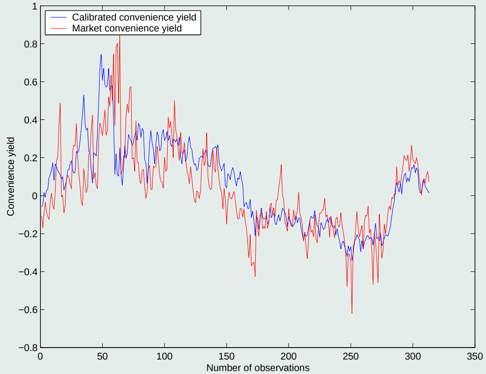

Figure 2: Comparison between filtered δ_{t_i} and market convenience yield, $\delta_{t_i}^{\text{market}}(\tau_1, \tau_2)$.

7. Errors

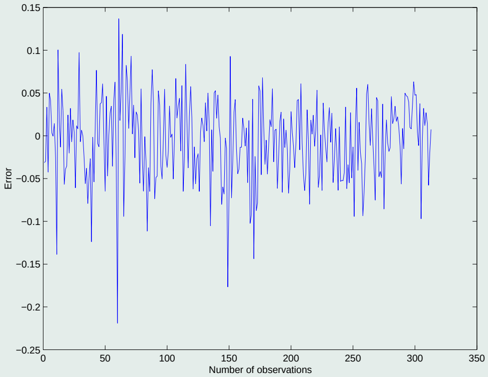

Figure 3: Innovation corresponding to $\mathbf{F}_t(\tau_1)$. Mean = -8.1734e-004, Variance = 0.0022.

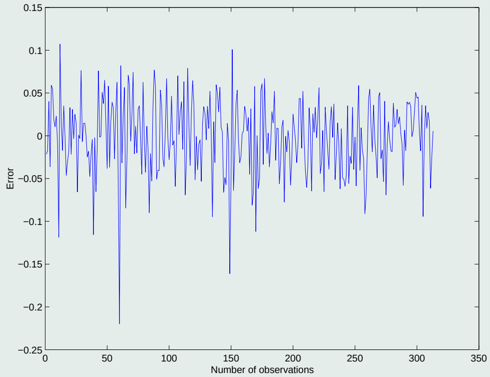

Figure 4: Innovation corresponding to $\mathbf{F}_t(\tau_2)$. Mean = 8.6078e-004, Variance = 0.0019.

8. Numerical results for the Cox-Ingersoll-Ross process for the commodity light crude oil

As noted earlier, the matrix $\mathbf{V}_{t_i}$ given in (9) depends on the state variables. This results in:

Parameters	Ini parset	Opti parset
k	1.4221	10.0000 (48.4424)
μ	0.3733	0.8616 (3.9825)
α	0.0699	1.1192 (3.1169)
λ	-0.0183	10.0000 (82.4541)
σ_S	0.3630	0.4219 (9.7882)
σ_δ	0.4028	10.0000 (7.8778)
ρ	0.8378	0.2196 (3.3102)
$\lvert h_1\rvert$	0.0246	0.0609 (0.0217)
$\lvert h_2\rvert$	0.0268	0.0382 (0.0108)
$\lvert h_3\rvert$	0.0291	0.0231 (0.0013)
$\lvert h_4\rvert$	0.0313	0.0109 (0.0031)
$\lvert h_5\rvert$	0.0336	0.0000 (0.0015)
$\lvert h_6\rvert$	0.0357	0.0096 (0.0016)
$\lvert h_7\rvert$	0.0377	0.0181 (0.0031)
Log-Likelihood		5104.3040

Table 2: Optimized parameter set (Opti parset) for different initial parameter sets (Ini parset). Standard errors in parentheses.

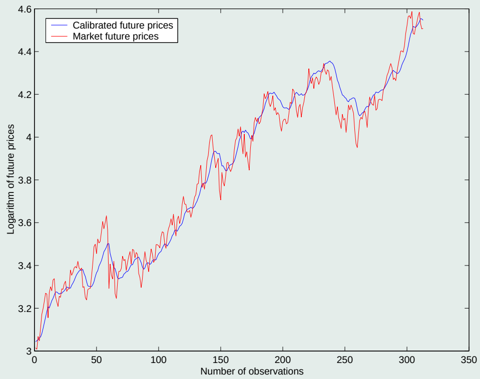

Figure 5: Comparison between the calibrated future prices and market future prices for contract τ_1.

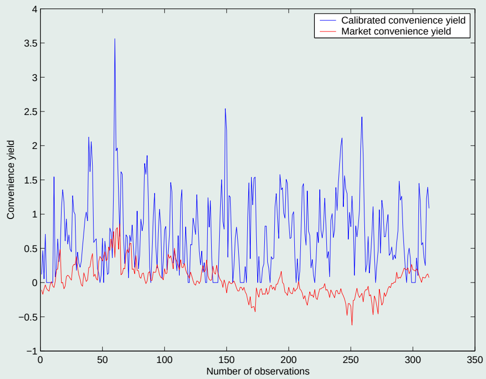

Figure 6: Comparison between the calibrated δ_t and the market implied convenience yield.

9. Improvements

If we shift the data such that $\delta_0^{\text{market}} > 0$ we have

Parameters	Ini parset	Opti parset	Ini parset	Opti parset	Ini parset	Opti parset
k	1.4221	1.6118 (0.0389)	2	1.6118 (0.0485)	1.4	1.6118 (0.0285)
μ	0.3733	0.2932 (0.1442)	0.5	0.2932 (0.1321)	0.2	0.2932 (0.1221)
α	0.0699	0.0590 (0.0973)	0.1	0.0590 (0.0843)	0.1	0.0590 (0.0880)
λ	-0.15	-0.1029(0.1571)	-0.1	-0.1029(0.1360)	0.2	-0.1029(0.1369)
σ_S	0.3630	0.5864 (0.0247)	0.3	0.5864 (0.0249)	0.5	0.5864 (0.0239)
σ_δ	0.4028	0.6598 (0.0274)	0.3	0.6598 (0.0249)	0.3	0.6598 (0.0262)
ρ	0.8378	0.8357 (0.1442)	0.4	0.8357 (0.0179)	0.6	0.8357 (0.0190)
$\|h_1\|$	0.0246	0.0189 (0.0008)	0.0246	0.0189 (0.0008)	0.1	0.0189 (0.0008)
$\|h_2\|$	0.0268	0.0073 (0.0003)	0.0268	0.0073 (0.0003)	0.1	0.0073 (0.0003)
$\|h_3\|$	0.0291	0.0022 (0.0001)	0.0291	0.0022 (0.0001)	0.1	0.0022 (0.0001)
$\|h_4\|$	0.0313	0.0000 (0.0001)	0.0313	0.0000 (0.0001)	0.1	0.0000 (0.0001)
$\|h_5\|$	0.0336	0.0006 (0.0000)	0.0336	0.0006 (0.0000)	0.1	0.0006 (0.0000)
$\|h_6\|$	0.0357	0.0000 (0.0001)	0.0357	0.0000 (0.0001)	0.1	0.0000 (0.0001)
$\|h_7\|$	0.0377	0.0015 (0.0001)	0.0377	0.0015 (0.0001)	0.1	0.0015 (0.0001)
Log-Likelihood		8341.0028		8341.0028		8341.0028

Table 3: Optimized parameter set (Opti parset) for different initial parameter sets (Ini parset). Standard errors in parentheses.

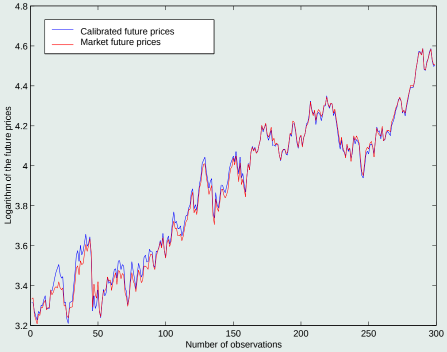

Figure 7: Comparison between the calibrated future prices and market future prices for contract τ_1.

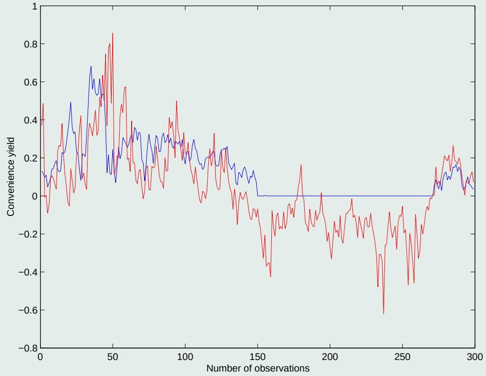

Figure 8: Comparison between the calibrated δ_{t_i} and the market convenience yield, $\delta_{t_i}^{\text{market}}(\tau_1, \tau_2)$.

10. Errors

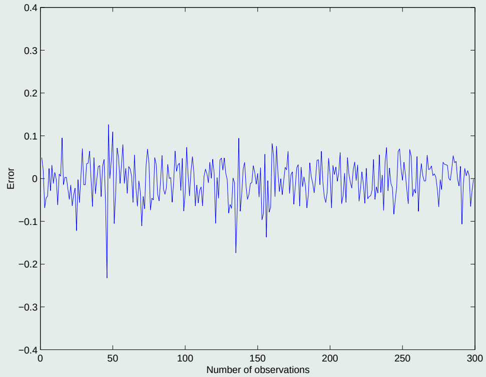

Figure 9: Innovation corresponding to $\mathbf{F}_t(\tau_1)$. Mean = -8.2412e-004, Variance = 0.0003.

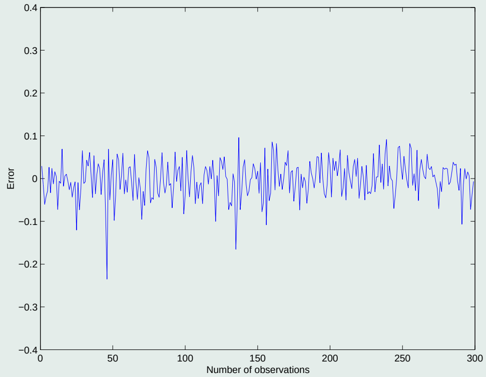

Figure 10: Innovation corresponding to $\mathbf{F}_t(\tau_2)$. Mean = 7.6238e-004, Variance = 0.0009.

11. Pricing put options on futures contracts

The value of a contingent claim V,where its payoff is given by a call i.e. $V(F,T) = \max(F-K)^+$, yields

$$V(F,t) = e^{-r(T-t)} F \mathcal{N}(d_1) - e^{-r(T-t)} K \mathcal{N}(d_2), \tag{10}$$

with

$$d_1 = \frac{\ln(F/K) + \frac{1}{2}\hat{\sigma}_F^2(T-t)}{\hat{\sigma}_F\sqrt{T-t}}, \quad d_2 = \frac{\ln(F/K) - \frac{1}{2}\hat{\sigma}_F^2(T-t)}{\hat{\sigma}_F\sqrt{T-t}}$$

and

$$\hat{\sigma}_F^2(t,T) = \frac{1}{T-t}\left\{\frac{2\rho\sigma_S\sigma_\delta}{k^2}(1-\theta) - \frac{2\rho\sigma_S\sigma_\delta}{k}(T-t) + \sigma_S^2(T-t) + \frac{\sigma_\delta^2}{2k^3}(1-\theta^2) - \frac{2\sigma_\delta^2}{k^3}(1-\theta) + \frac{\sigma_\delta^2}{k^2}(T-t)\right\}. \quad (1$$

12. Contract details

Contract	Date at t=0	Date at t=T	Last obs. day	Observed trading days	Total trading days
M8	20/11/2007	20/05/2008	17/03/2008	79	125
Z8	20/11/2007	20/11/2008	17/03/2008	79	258
M9	20/11/2007	19/05/2009	17/03/2008	79	386

Table 4: Contract details.

13. Results following a naïve approach

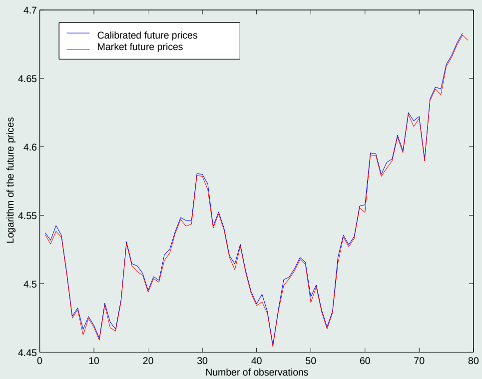

Figure 11: Comparison between the calibrated future prices and market future prices for contract M8.

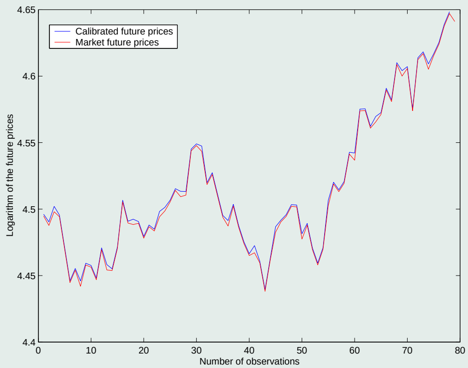

Figure 12: Comparison between the calibrated future prices and market future prices for contract Z8.

Parameters	Ini parset	Opti parset
k	1.4221	0.8046 (0.1012)
μ	0.3733	0.5374 (0.4453)
α	0.0699	0.0851 (0.0169)
λ	-0.0183	-0.0754(0.1405)
σ_S	0.3630	0.3493 (0.0305)
σ_δ	0.4028	0.1981 (0.0234)
ρ	0.8378	0.7171 (0.0593)
$\|h_1\|$	0.0341	0.0000 (0.0005)
$\|h_2\|$	0.0300	0.0000 (0.0005)
$\|h_3\|$	0.0291	0.0027 (0.0002)
Log-Likelihood		902.7301

Table 5: Optimized parameter set (Opti parset). Standard errors in parentheses.

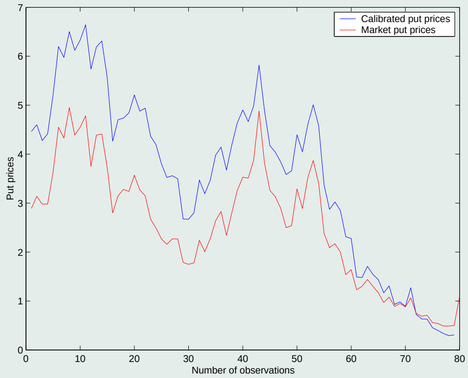

Figure 13: Comparison between the calibrated put prices and market put prices for contract M8 with K=85.

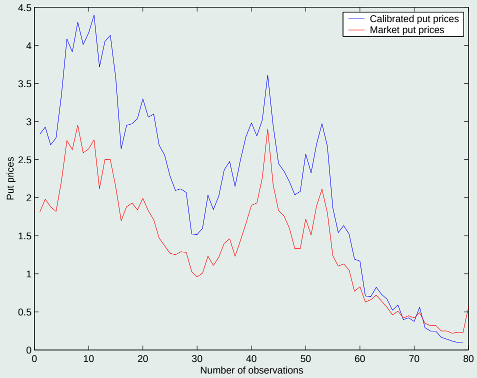

Figure 14: Comparison between the calibrated put prices and market put prices for contract M8 with K=80.

14. Results for a matured M8 contract for different strikes

Contract	K	Date at t=0	Date at t=T	Observed trading days	Total trading days
M8	K= 85	20/11/2007	20/05/2008	125	125
M8	K=110	05/12/2007	20/05/2008	115	115
M8	K=115	10/03/2008	20/05/2008	51	51
M8	K=125	13/03/2007	20/05/2008	48	48

Table 6: Contract details.

Parameters	K=85	K=110	K=115	K=125
k	0.2089	0.2144	0.0014	0.0630
μ	1.4354	1.3117	6.5556	3.9980
α	11.2299	8.0303	0.2753	109.2796
λ	3.1413	1.9467	7.5792	18.3986
σ_S	0.2613	0.2587	0.3013	0.1649
σ_δ	0.0303	0.0455	3.0048	1.6310
ρ	0.9999	0.9999	0.6635	-0.9999
$\lvert h_1 \rvert$	0.0341	0.0231	0.0013	0.0320

Table 7: Optimized parameter set for different strike prices for the contract M8.

Parameters	K=85	K=110	K=115	K=125
σ_S	0.3737	0.3756	0.3090	0.2415
σ_δ	0.6701	0.4923	3.8011	1.7195
$\lvert h_1 \rvert$	0.0145	0.0159	0.0056	0.0265

Table 8: Optimized parameter set for different strike prices for the contract M8.

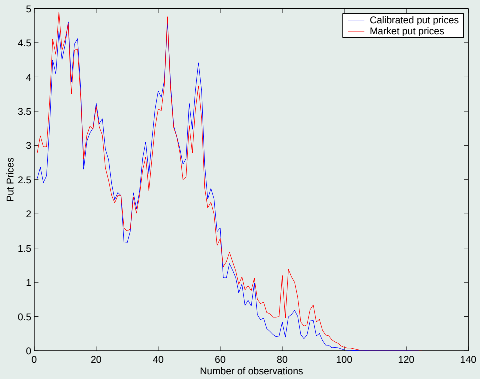

Figure 15: Comparison between the calibrated put prices and market put prices for contract M8 K=85.

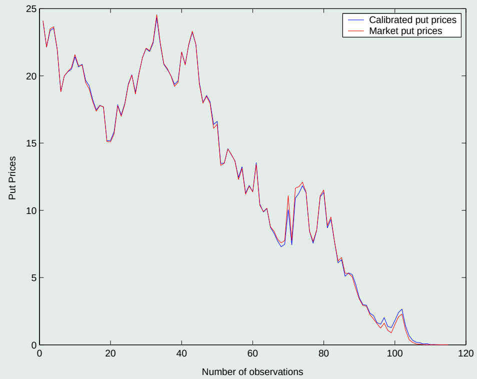

Figure 16: Comparison between the calibrated put prices and market put prices for contract M8 K=110.

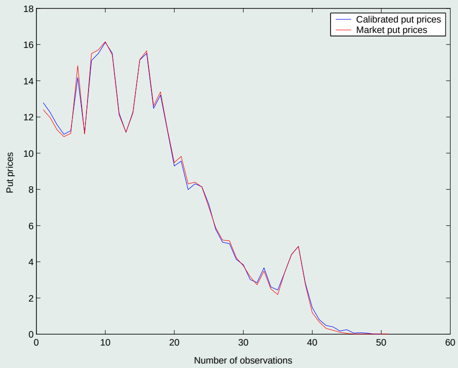

Figure 17: Comparison between the calibrated put prices and market future put for contract M8 K=115.

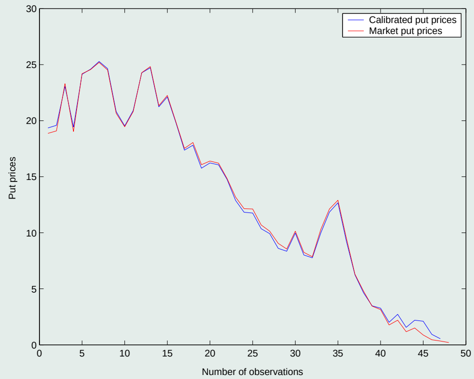

Figure 18: Comparison between the calibrated put prices and market future put for contract M8 K=125.

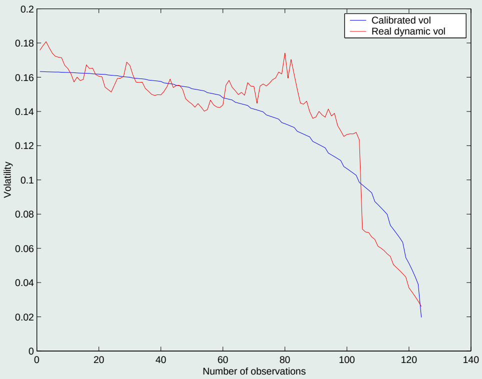

Figure 19: Comparison between $\tilde{\sigma}_F(t,T)$ and $\sigma_{\mathrm{RD}}(t,T)$ for contract M8 with K=85.

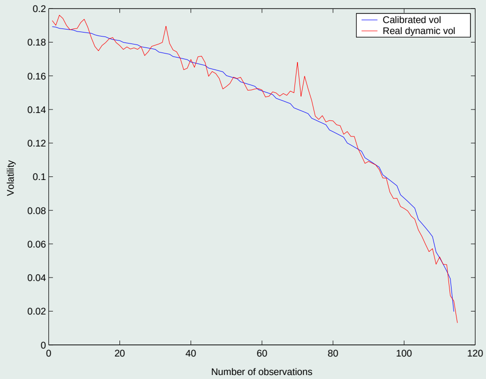

Figure 20: Comparison between $\tilde{\sigma}_F(t,T)$ and $\sigma_{\mathrm{RD}}(t,T)$ for contract M8 with K=110.

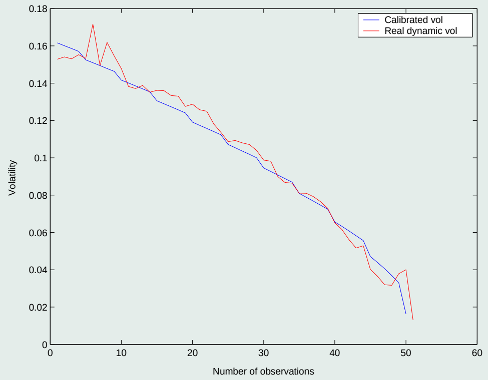

Figure 21: Comparison between $\tilde{\sigma}_F(t,T)$ and $\sigma_{\mathrm{RD}}(t,T)$ for contract M8 with K=115.

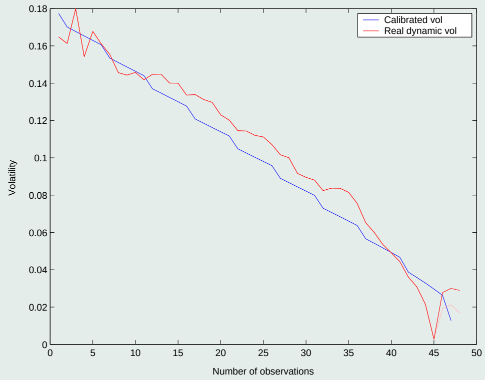

Figure 22: Comparison between $\tilde{\sigma}_F(t,T)$ and $\sigma_{\mathrm{RD}}(t,T)$ for contract M8 with K=125.

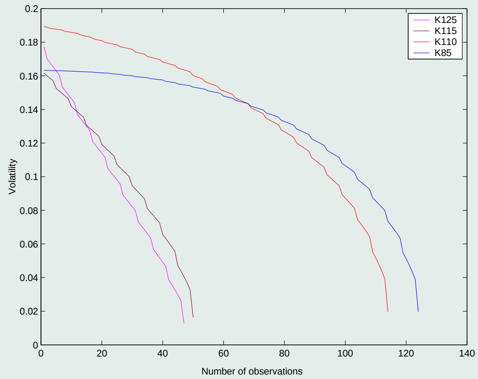

Figure 23: Calibrated volatility contract M8 with different strike prices

15. Results for unmatured contracts

Ideas:

- $\sigma_S = \bar{\sigma}_S \tau^\beta$ and $\sigma_\delta = \bar{\sigma}_\delta \tau^\gamma$ to include more (time-dependent) structure into (11)
- $\tilde{\sigma}_F = a^2\tau^b + c^2\tau^\gamma + d^2, \quad \gamma \leq 0,$

Results

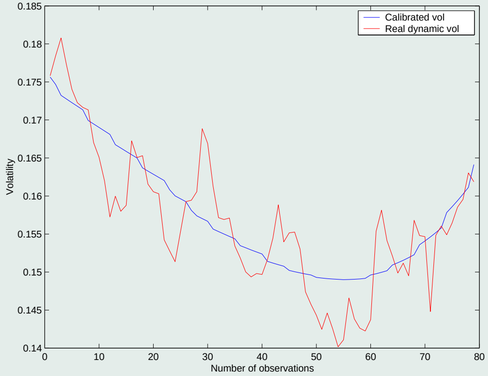

Figure 24: Comparison between $\tilde{\sigma}_F(t,T)$ and $\sigma_{\mathrm{RD}}(t,T)$ for contract M8 with K=85.

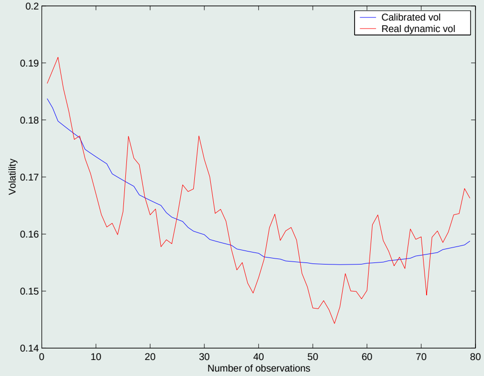

Figure 25: Comparison between $\tilde{\sigma}_F(t,T)$ and $\sigma_{\mathrm{RD}}(t,T)$ for contract M8 with K=80.

16. Discussion

- Although the EKF is not optimal for the Ornstein-Uhlenbeck process, it is still acceptable and therefore we use this technique to price put options on futures contracts.

- Inadequacy of the CIR process.
  - CIR process was inspired by Robeiro and Hodges.
  - Period from 17^{th} of March 1999 to the 24^{th} of December 2003.
  - 20 observations.

- Initial values of the parameters unknown.
  - Tested [10,-10].
  - Converged to the same optimized parameter set.

- When pricing a put option on a futures contract, there are some important details to be considered.

  - Stochastic interest rates.

  - The errors in our calibrated put prices can be explained by the use of the extended Kalman filter. When linearizing the system matrices, we introduce an approximation in the estimation.

High values of some parameters. What could be concluded?

17. Further research

Topics of further research are

- Starting from the future process, one does not know how to choose this volatility. In fact, the future price process may be given by

$$\frac{dF(t,T)}{F(t,T)} = \sum_{i=1}^{n} \sigma_i dW_t^i,$$

  with i-independent Brownian motions.
  Choose

$$\frac{dF(t,T)}{F(t,T)} = \sigma_1(t,T)dW_t^1 + \sigma_2(t,T)dW_t^2, \tag{12}$$

  with

$$\sigma_1(t) = \sqrt{1-\rho^2}\sigma_S \quad \text{and} \quad \sigma_2(t) = \rho\sigma_S \tag{13}$$

  and

$$\begin{cases} W_t^1 = \dfrac{W_t^S}{\sqrt{1-\rho^2}} - \dfrac{\rho W_t^\delta}{\sqrt{1-\rho^2}}, \\ W_t^2 = W_t^\delta. \end{cases} \tag{14}$$

Then

$$\frac{dS_t}{S_t} = (r - \delta_t)dt + \sigma_S dW_t^S \tag{15}$$

and

$$d\delta_t = k(\alpha(t) - \delta_t)dt + \sigma_\delta dW_t^\delta, \tag{16}$$

with

$$\alpha(t) = \frac{1}{k}\frac{\partial^2}{\partial t^2}\ln F(0,t) + \frac{\partial}{\partial t}\ln F(0,t) + \frac{\sigma_\delta^2}{2k^2}(e^{-2kt} - 1) + \frac{\rho\sigma_S\sigma_\delta}{k}. \tag{17}$$

- Another reason for initially assuming stochastic processes for the state variables is because of the Greeks.

- High values of parameters. Solutions:
  - accept
  - stochastic volatility
  - jump processes
  - time-dependent mean-reverting term
- Economic, weather, war.

18. Conclusion

It is a real challenge to end up with a realistic model for oil prices which, at the same time, can be dealt with in a fast and efficient way. The models presented in this work are a first step in that direction.